Available online at www.sciencedirect.com
ScienceDirect
Catalysis Today 126 (2007) 211–218
CATALYSIS TODAY
www.elsevier.com/locate/cattod

Influence of annealing temperature on the CO sensing mechanism for tin dioxide based sensors–Operando studies

D. Koziej [a,b,*], K. Thomas [c], N. Barsan [a], F. Thibault-Starzyk [c], U. Weimar [a]

[a] *Institute of Physical and Theoretical Chemistry, University of Tübingen, Germany*
[b] *Department of Electron Technology, Silesian University of Technology, Gliwice, Poland*
[c] *Laboratoire Catalyse & Spectrochimie, CNRS-ENSICAEN-Université de Caen, France*

Available online 17 April 2007

Abstract

In this work, we made an attempt to understand the influence of the annealing treatment on CO sensing with tin dioxide based sensors. As a first step, the surface of tin dioxide powders and of sensitive layers based on them has been characterised by means of the IR studies; it was shown in this way that at the surface of thick film SnO_2 based sensors the structure of hydroxyl groups is similar to the one found at the surface of SnO_2 powders, independent on the sensors' annealing temperature. Afterwards, the CO reaction with sensors annealed at 500 and 700 °C has been investigated by simultaneous electrical and infrared studies (DRIFTS) in operando conditions (air, 200–400 °C). It was concluded that the final annealing temperature influences the concentration of the reactive sites for oxygen ionosorption, which finally determines the main CO reaction route and thus the sensor signal.

Keywords: Operando; SnO_2; CO; Gas sensors; Annealing temperature

1. Introduction

Spectroscopic techniques are extremely powerful for characterising metal oxide, in general, since they can provide, e.g. details about the active surface sites and insight into the reaction processes. For tin oxide, basic spectroscopic studies of surface properties have been frequently performed in the past three decades [1–3]. Recently, having catalytic and sensing application in mind, Amalric-Popescu and Bozon-Verduraz [4] after thoroughly reviewing the available literature made an attempt to establish the present state of the art in the field of the influence of the pre-treatment (temperature, oxygen background) on the properties of tin dioxide powders. However, experiments have always been performed under static conditions (exposure) or after outgassing/evacuation, which mismatches with the optimal conditions for measuring sensors performance.DRIFT experiments have been already performed in the past for the characterisation in real conditions of powders [5–8] and of real sensors; the latter were even performed at sensors' working temperatures [9–12]. Generally, during the gas sensing process with metal oxide based sensors the determining factors are the different ways by which charge carriers are exchanged with the conduction band of the sensing material because of the usual manner in which the effects are recorded, id est by measuring the resistance changes upon gas exposure [13]. This is different from the case of catalysis where the target is simply the conversion of a molecule into another one [14] and the process lets the catalyst unchanged. Besides the reaction participants that are exchanging charge carriers with the conduction bands, there are also other ''participants'' to sensing process, the so-called spectators. Their effect is not recorded as resistance changes. They are either: (a) surface species present at the surface during gas exposure that do not actively take part in the reaction. But can have indirect influence on the reaction by, e.g. blocking the active sites; or (b) species which formation involves localised charge transfer processes that determine only changes of the metal oxide electron affinity ($\Delta\chi$) and by that are not recorded as signals.

When one simultaneously perform DRIFT spectroscopy and electrical measurements (truly operando) on sensors it is even possible to correlate changes in the surface species with electrical

* Corresponding author at: Institute of Physical and Theoretical Chemistry, University of Tübingen, Germany.
E-mail address: dorota.koziej@ipc.uni-tuebingen.de (D. Koziej).

0920-5861/$ – see front matter © 2007 Published by Elsevier B.V.
doi:10.1016/j.cattod.2007.03.011

properties of the solid. This fact is of fundamental importance for the modelling of gas sensing reactions because the sensing process is known to be very complex. The whole of the sensor is involved, with electrodes, substrate, and most important their interface to the actual 'sensing material'. It was shown, for example, by varying the thickness of the sensitive layer that CO sensing with Pd doped thick film tin dioxide does take place mostly at the four phases boundary substrate/electrodes/tin dioxide/atmosphere [15,16]. The high sensitivity to surface species, combined with an important light penetration depth, allow DRIFT spectroscopy to acquire data containing information from all relevant components. Some downsides exist nevertheless for direct measurements on the working sensor:

- The spectroscopic information is slightly delocalised because it is not possible to distinguish between the different regions of the sensors (sensing layers).
- One generally needs to work with ''difference'' spectra (with the reference spectra recorded directly before gas exposure) that contain only information about the surface species actively taking part in the sensing. No absolute information on the state of the surface can be derived this way, and species influencing the sensing process only indirectly will not be identified.

In order to compensate for these disadvantages we need to supplement the DRIFTS studies on sensors with, e.g. IR measurements on powders and on the alumina substrate itself. In any ways, the information one is able to derive from DRIFTS on sensors is much richer than what one can derive by measuring powders and the other sensor components separately because the sensor effect is not the algebraic sum of its components.

CO sensing with tin oxide based sensors is the topic of many studies [2,4,13,17–21]; one generally agrees that the ionsorbed oxygen species are CO reaction partners, different carbonates and carboxylates are reaction intermediates and that the final reaction product is CO_2. It is quite amazing in fact, that one does not have a full understanding of such a ''simple'' sensing process. Much seems to depend on the specifics of the individual experiments: (a) pre-treatment (temperature, background gases, sensors history) and (b) operation conditions (humidity, low oxygen concentration, temperature). This very fact points towards the lack of understanding of the role of sample/sensors preparation parameters in determining the sensing performance.

In this paper, we focus on the role of the final sensor thermal treatment on CO sensing. In doing so we are using the following approach:

- Firstly, we compare surface properties of tin dioxide powders under vacuum or low pressure (in situ IR transmission spectroscopy of adsorbed probe molecules) with spectroscopic observations of tin dioxide based sensors in working conditions (DRIFTS on the same powders).
- Secondly, we compare CO sensing performance of sensors thermally treated at 500 and 700 °C by DRIFTS measurements.

2. Experimental

The SnO_2 powders were prepared by hydrothermal treatment. The hydrothermal treatment of sol solution of tin oxide is known to suppress the grain growth when they are subjected to further thermal treatments. Therefore, this method has been selected in order to ensure the thermal stability of the SnO_2 grains size. An extensive description of the procedure can be found elsewhere [22].

In the gas sensing experiments, real sensors were used. They were obtained by screen printing SnO_2 based pastes (followed by an annealing step) onto α-Al_2O_3 substrate plates with Pt electrodes and heaters. During the final annealing process (firing) of the sensors, the organic binders of the film are fully removed. The solvent used in this study for the paste preparation volatilises rapidly at temperatures around 100–150 °C. The sensors are gradually heated up to the maximal temperature of 500 or 700 °C, maintained at this temperature for 10 min and finally gradually cooled down to RT. Sensors annealed at different temperatures are denoted in the following by T500 and T700, respectively.

The tin dioxide is an n-type semiconductor with a wide band gap equal to 3.6 eV. The n-type behaviour originates from its native non-stoichiometry caused by oxygen vacancies. The concentration of surface point defects (oxygen vacancies) increases with temperature [23]. Those two specific sensors' annealing temperatures have been chosen because it was shown that a temperature of at least 450 °C is needed to start the process of desorption of surface lattice oxygen [18] while at temperatures higher than 600 °C, desorption of bulk lattice oxygen becomes possible [24]. Kappler et al. [25,26] observed that annealing of the sensors do not influence the morphology (grain size, porosity, etc.). Our gain in this case is clear—by having a fixed morphology, the microstructure of tin dioxide based sensors is changed in a controlled way.

For gas sensing experiments, all gas mixtures were fed at 200 ml/min. The carrier gas was air. During the experiments the residual water was trapped by a liquid nitrogen trap and the humidity level was monitored by using a dew point meter (Alpha Moisture System DS 1000). The CO sensing mechanism was investigated by simultaneous diffuse reflectance infrared Fourier transformed spectroscopy (Bruker 66v FTIR spectrometer) and resistance measurements (Keithley 617).

The sensors have been operated at temperatures between 200 and 400 °C. At this temperature range all bulk oxygen vacancies are believed to be double ionised [18,27] and it can be ensured that within the experimental run no changes of the concentration of bulk oxygen vacancies takes place [24,28,29].

3. Results and discussion

3.1. Material characterisation

3.1.1. Infrared spectra of tin dioxide powders, D_2O exchange

Fig. 1(a) shows the spectrum of activated (by heating at 100 °C in 20 Torr of oxygen) SnO_2 powder. Several features can be identified in this spectrum (detailed in Table 1):

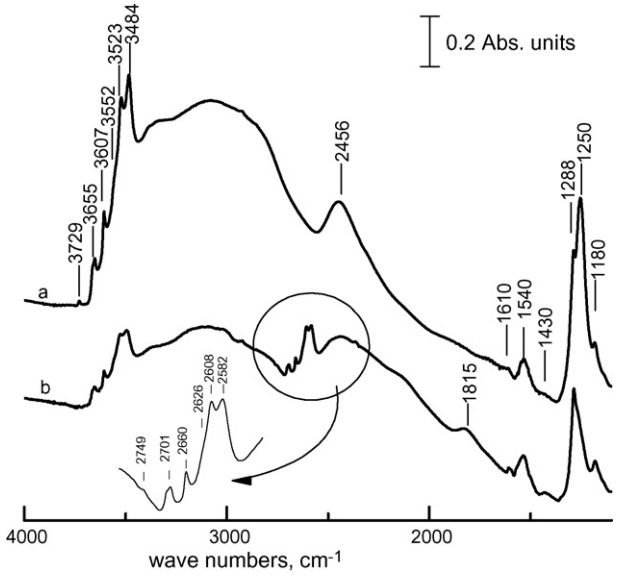

Fig. 1. (a) Spectrum of the SnO_2 pellet (18.01 mg) activated at 100 °C and 20 Torr of oxygen. (b) Spectrum of the SnO_2 pellet after exposure of 1 Torr of D_2O. Spectra were recorded at RT.

- ν(OH) vibration bands for free OH groups, between 3750 and 3480 cm^{-1};
- Strongly H-bonded OH groups, with the typical A,B pattern (strong and broad bands at 3000 and 2500 cm^{-1} with a so-called Evans' window in the middle). The H-bonded species manifest themselves as a broad band in the range from 3400 up to 2000 cm^{-1}. Its center varies strongly on different samples (i.e. 3300 and 3700–2000 cm^{-1} [30], 3000 cm^{-1} [31], 3500–2500 cm^{-1} [32]) and often is disturbed by an apparent band at ca. 2450 cm^{-1} (2δ(OH)). This spectral feature is called Evans' window. Its formation is a consequence of Fermi resonance, when a very broad stretching ν(OH) vibration band of associated hydroxyls overlaps the (very narrow and weak) overtone band of the deformation vibration 2δ(OH) [32,33]. The shape of the resulting feature depends on the strength of association (strength of H-bond) [34];
- δ(OH) vibration band at 1288, 1250 and 1180 cm^{-1}.

Table 1
Correlation table of water related species and corresponding heavy water related species at the surface of tin dioxide powder

νOH (cm^{-1})	νOD (cm^{-1})	OH/OD ratio
3729	2749	1.356
3655	2701	1.353
3607	2660	1.356
3552 (vw)	2626 (vw)	1.356
3523	2608	1.351
3483	2582	1.349
Evans' window OH (cm^{-1})	Evans' window OD (cm^{-1})	OH/OD ratio
2456	1815	1.353
δOH (cm^{-1})	δOD (cm^{-1})	OH/OD ratio
1288	–	–
1250	–	–
1180	–	–

'vw' stands for very weak.

Band assignment is confirmed by isotopic exchange reaction with gaseous D_2O, which yields the second spectrum shown in Fig. 1(b). The OH/OD ratio is 1.353 ± 0.003. It was not possible to observe the shift of the deformations mode of the hydroxyl groups due to the lack of transparency of the CaF_2 windows in the region below 1100 cm^{-1}. But the decreases of the intensity of those bands are evident (range 1300–1100 cm^{-1}).

Additionally, three bands at 1610, 1540 and 1430 cm^{-1} have been observed. Those bands intensity and positions are not influenced by D_2O exposure.

3.1.2. Characterisation of surface of powders and the sensors in flow of air and at different temperatures

In Fig. 2(a) the spectrum of pure SnO_2 (self supporting wafer) is compared to those of two sensors (SnO_2 on alumina support, with platinum heater and connections, annealed at 500 or 700 °C – b and c, respectively) under air at RT. The ν(OH) band at 3729 cm^{-1} is present on all samples, with or without alumina, and can clearly be assigned purely to SnO_2, and not to alumina [10] or to the SnO_2/Al_2O_3 interface. Additionally, the overall decrease of the intensity of water related species suggest the higher surface dehydroxylation stage of the sensor annealed at 700 °C.

The following discrepancies between the spectra of tin dioxide powder and of tin dioxide based sensors have been observed:

- In the spectra of both sensors the vibration of gaseous CO_2 (2350 cm^{-1}) localised in the pores of alumina substrate [10] and deformation mode of physisorbed water (1640 cm^{-1}) are observed.

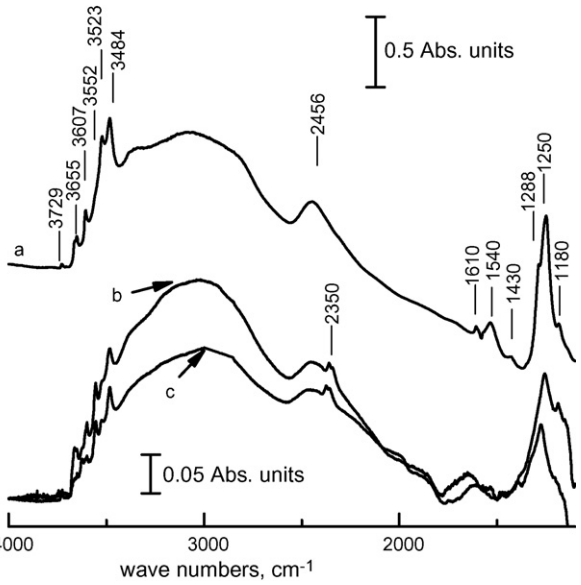

Fig. 2. Comparison of the IR spectra of tin dioxide pellet (a) with two sensors annealed at 500 °C (b) and 700 °C (c), at RT in the flow of air.

- In the spectrum of the pure powder, bands at 1610 (very weak) 1540 and 1430 cm^{-1} have been observed not to be sensitive to D_2O exposure. While some authors believe that the two former bands belong to surface bridging oxygen [1,35], it is difficult to understand why they should disappear after the oxygen treatment at 200 °C (observed for the first time by Ref. [4] and confirmed within this work – for the sake of clarity spectra are not included here), and additional work seems necessary for a definite assignment.

No bands which could clearly be assigned to ionosorbed oxygen (O_2^-) have been observed. There are several FTIR studies devoted to oxygen adsorption at the surface of tin dioxide [20,36] but there is no common agreement upon evidence of the O_2^- in the IR spectra, probably because these species manifest themselves in the same spectral range as the lattice combination SnO_2 modes and the deformation vibration of hydroxyl groups. While the observation of the O_2^- is disputable, the O^- is not expected to lead to any infrared absorption.

The following surface oxygen species have been evidenced previously with other spectroscopic techniques on the surface of tin dioxide: at lower temperatures (<150–200 °C) oxygen adsorbs on SnO_2 non-dissociatively in a molecular form (either neutral $O_{2(ads)}$ or charged $O_{2(ads)}^-$), and at higher temperatures it dissociates into atomic oxygen (either neutral $O_{(ads)}$ or charged $O_{(ads)}^-$) [13,37].

4. Simultaneous DRIFT and resistance measurements on sensors

4.1. Spectroscopic insights

4.1.1. CO sensing at 200 °C

Figs. 3–6 depict the changes of the surface species upon exposure to different CO concentrations. The maxima represent an increase of band intensities, and thus of surface species concentrations (intermediates or products), while minima represent a decrease of spectroscopic intensities, and of surface species concentrations (educts). On the surface of sensors under a CO flow, the following bands have been observed. (a) Sensor annealed at 500 °C (T500): two well resolved bands at 1440 and 1372 cm^{-1} and small shoulders at 1530, 1495, 1330 cm^{-1}, (b) sensor annealed at 700 °C (T700): 1545, 1520, 1440, 1372, 1320 cm^{-1}. In all cases the concentration of the surface species depends on CO concentration. The band position and assignments are given in Table 2.

IR bands for surface species on oxides are usually assigned by analogy with the corresponding bulk structures [38]. Special attention has to be paid, because different forms of ionised oxygen are considered to be the reaction partners for CO on the tin dioxide surface, and not an oxygen atom, as commonly assumed in IR studies on metal oxides. This may have an influence on shape and bands position. Additionally, in the case of sensors T700, strong modification of the baseline absorbance has been observed.

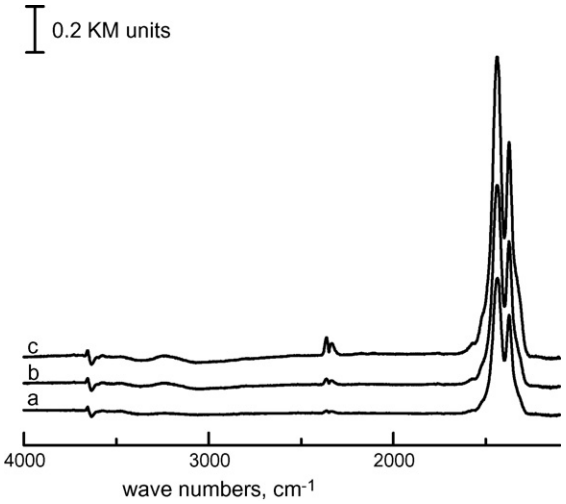

Fig. 3. DRIFT spectra of the sensors annealed at 500 °C exposed to 50, 100, 250 ppm of CO at 200 °C. As a reference spectrum in air directly before CO exposure has been used.

The comparison of the spectra of the two sensors, together with relative intensities of individual bands, brings about the following conclusions:

- Sensor annealed at 500 °C (T500) – the main CO reaction with tin dioxide appears to be the one which involve CO_3^- as the intermediates, and not CO_3^{2-} and CO_2^-.
- Sensor annealed at 700 °C (T700) – the spectra is much more complex. All visible bands on the sensors annealed at 500 °C are now reaching the same intensity as the bands assigned to CO_3^- (1440 and 1370 cm^{-1}). Thus, CO_2^- and CO_3^{2-} concentrations were increased with respect to CO_3^-. Additionally, a new type of carbonates (CO_3) is observed. It suggests that an increase of annealing temperature increases the reaction partners/sites for their formation.

CO_3^- and CO_2^- could be intermediate species in CO to CO_2

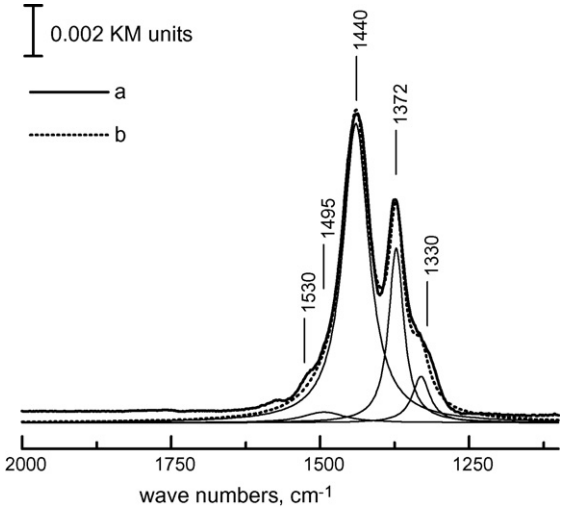

Fig. 4. Results of peak fitting procedure in the spectral range characteristic for carbonates and carboxylates vibrations (fit of the spectra at 250 ppm of CO) of the sensors annealed at 500 °C. The Gaussian function was used in order to fit separate bands.

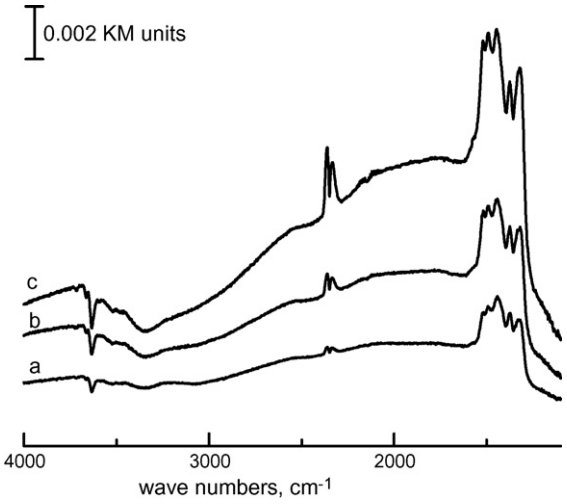

Fig. 5. DRIFT spectra of the sensors annealed at 700 °C exposed to 50, 100, 250 ppm of CO at 200 °C. As a reference spectrum in air directly before CO exposure has been used.

conversion on the surface of tin dioxide based sensors according to the following reactions:

$$CO + O_2^- \rightarrow CO_3^- \quad (1a)$$

$$CO_3^- + CO \rightarrow 2CO_{2gas} + 1e^- \quad (1b)$$

$$CO + O^- \rightarrow CO_2^- \quad (2a)$$

$$CO_2^- \rightarrow CO_{2gas} + 1e^- \quad (2b)$$

Furthermore, an increase of free (noncoordinated) carbonates concentration is also observed. They are known to have the highest thermal stability upon all surface carbonates [39]:

$$CO + 2O^- \leftrightarrow CO_3^{2-} \quad (3)$$

$$CO + O_2^- + 1e \leftrightarrow CO_3^{2-} \quad (4)$$

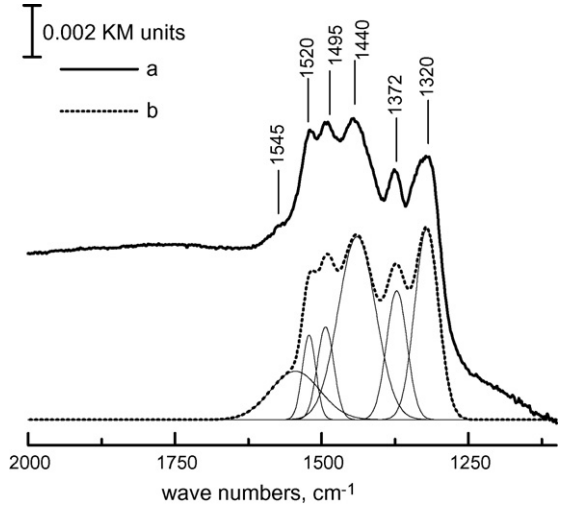

Fig. 6. Results of peak fitting procedure in the spectral range characteristic for carbonates and carboxylates vibrations (fit of the spectra at 250 ppm of CO) of the sensors annealed at 700 °C. The Gaussian function was used in order to fit separate bands. The baseline was corrected.

Table 2
Correlation table for the assignment of the absorption bands in DRIFT spectra of different surface carbonates, carboxylates

Type of compound	ν (cm^{-1}), T500	ν (cm^{-1}), T700
CO_3^-	1440 (ν_{as} COO) 1372 (ν_s COO)	1440 (ν_{as} COO) 1372 (ν_s COO)
CO_3^{2-}	1495 (ν_{as} COO)	1495 (ν_{as} COO)
CO_3	– –	1545 (ν C═O) 1320 (ν_{as} COO)
CO_2^-	1530 (ν_{as} COO) 1330 (ν_s COO)	1520 (ν_{as} COO) 1320 (ν_s COO)
$HO–CO_2^-$	–	–

Finally, CO_3 species are observed; It was shown that the partners for their formation are surface lattice oxygen [40] and not ionosorbed oxygen. Their formation was observed even when there was no oxygen in the ambient gas and they do not induced CO_2 formation [40,41].

$$CO + 2O_{latt} \leftrightarrow CO_3 \quad (5)$$

Changes in oxygen vacancies concentration lead to varying concentrations for different forms of oxygen, and thus also to different CO reaction pathways.

The intensities of ν(OH) bands decrease during the formation of different forms of carbonates and carboxylates on the surface of both tin dioxide based sensors. However, the behaviour differs qualitatively from sensor to sensor. In the case of the sensor T500 a complex behaviour has been observed.

In order to analyse the origins of observed changes we compare a row data (single channel spectra – Fig. 7) to the calculated on their bases Kubelka Munk spectra (spectra—Fig. 8).

Single channel spectra of the sensor in air and at 200 °C show, among others, bands at 3663 and 3643 cm^{-1}. CO exposure induces certain changes of these two bands: a clear decrease of the band at 3643 cm^{-1} and a broadening of the band at 3663 cm^{-1}. In the broadening of the second band in KM representation a maximum at 3655 cm^{-1} appears.

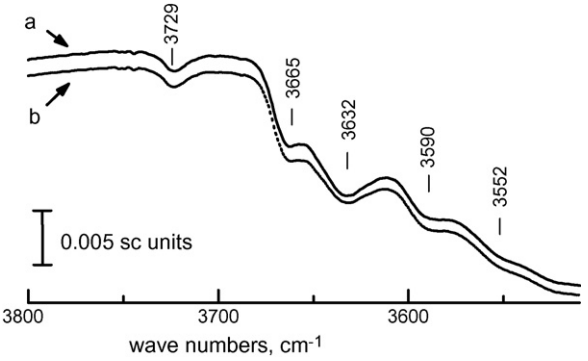

Fig. 7. DRIFT spectra of T500 sensor exposed to 50 ppm of CO in air at 200 °C. Single channel spectra: a – in air; b – in 50 ppm of CO.

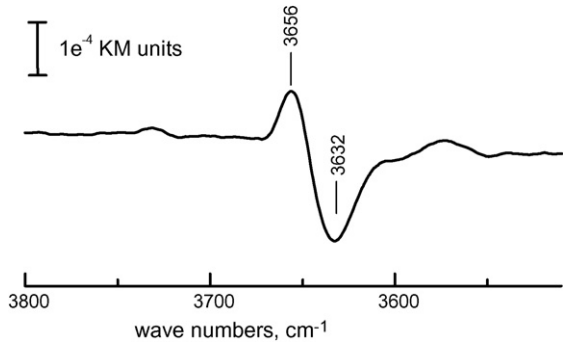

Fig. 8. DRIFT spectra of T500 sensor exposed to 50 ppm of CO in air at 200 °C. The difference spectrum in Kubelka Munk units where the spectrum before CO exposure in air was used as a reference.

In the case of the sensor T700 the CO exposure induces decreases of all OH groups but the band at 3643 cm^{-1} decrease foremost.

The decrease of the OH groups induced by CO exposure can be explained either through a direct or an indirect reaction. In the case of direct reaction between hydroxyl groups and CO an intermediates species should be observed $HCOO^-$ or $HOCOO^-$. However, there are no evidences for the formation of these species: the first one (formates) would, additionally to the COO^- bands (which might overlaps with other carbonates), show a νCH vibration at ~3000 cm^{-1}, while the former one (bicarbonates) would manifest themselves as νOH at 3600, δOH at 1220, νCO at 1700 cm^{-1}. Both of them are known to be unstable at temperatures slightly above RT.

Therefore, we believe that the decrease of the hydroxyl groups is a side effect induced by a decrease of oxygen ions concentration [42]. As, in this specific condition, the observed changes are not very strong, the hydroxyl groups are consider to play a minor role in CO sensing. For the sake of simplicity, within this work, they are not included in the modelling of CO reaction at the surface of the tin dioxide based sensors.

4.1.2. CO sensing at 300 and 400 °C

At 300 °C the same spectral features, but less intensive when compared to the 200 °C case, are observed, while at 400 °C only gaseous CO_2 is observed with no trace of surface intermediates. The latter could be a follow up of: (a) the thermal instability of the surface intermediates [38] and/or (b) saturation of the MCT detector [43]. At this temperature an additional reaction at the surface of tin dioxide not mentioned until now, becomes possible (reaction with double ionised oxygen):

$$CO + O^- \rightarrow CO_2 + 2e^- \quad (6)$$

The DRIFT spectra of CO sensing at these two temperatures was not shown for the sake of clarity.

4.2. Sensors performance

The changes of the conductance upon CO exposure and the resulting sensor signals are shown in Figs. 9 and 10, respectively. The sensor T500 shows the highest sensor signal (the relative increase of the conductance upon CO exposure) at 200 °C and, with the increase of the sensor's working temperature, the signal decreases. Differently, for the sensor T700, the highest sensor signal was measured at 300 °C.

When it comes to the sensitivity (slope of the calibration curve), the following clear trends are observed:

- For both sensors, the sensitivity has a marked maximum at 300 °C.
- For all operation temperatures the sensitivity of the sensor T700 is lower than the one of the sensor T500.

The interpretation of the electrical data is complicated by the fact that the adsorption of both reaction partners, oxygen ions and CO, depends on the temperature. As it was already mentioned the increase of temperature determines the type of surface oxygen species; that one determines the value of the exponent n from the experimentally observed dependence of conductance on the concentration of CO:

$$G \approx \text{const} \times P_{CO}^{n} \quad (7)$$

The value of n depends on the form of reactive oxygen according to the following scheme $n(O_2^-) > n(O^-) > n(O^{2-})$ [37]; keeping in mind the fact that its value directly influences the sensitivity – higher n means higher sensitivity – one can say that a dominant O_2^- reaction mechanism will result in a higher sensitivity than a dominant O^- mechanism. This is not valid for the sensor signal that will mainly depend on the value of the const parameter in Eq. (7); this one will depend on the different

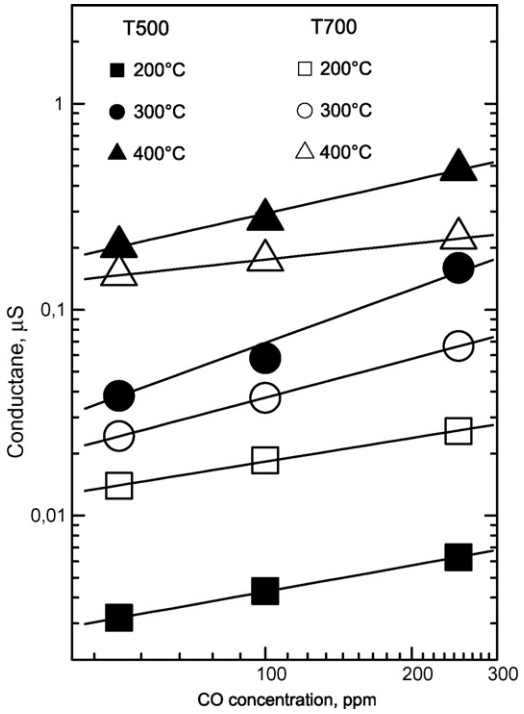

Fig. 9. Conductance changes induced by exposure of CO in the range from 50 to 250 ppm at 200 °C working temperature. In the graphic additionally to the values of the conductance the standard deviations from the mean value as an error bars have been included. However, in the most of the cases they are smaller than the size of the measurements symbols and therefore not visible.

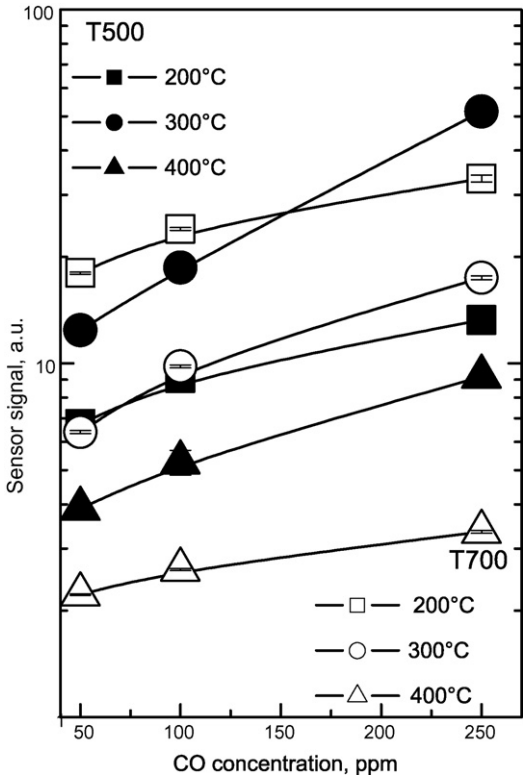

Fig. 10. Sensor signal induced by exposure of CO in the range from 50 to 250 ppm at 200 °C working temperature. In the graphic additionally to the values of sensor signal the standard deviations from the mean value as an error bars have been included. However, in the most of the cases they are smaller than the size of the measurements symbols and therefore not visible.

activation energies of the reaction processes with different oxygen ionosorbed species. From this point of view the oxygen species-sensitivity sequence will not be valid anymore when we are examining the sensor signal. The additional factor we need to consider is the availability of adsorbed CO for the reaction; due to the fact that the concentration of CO at the surface decreases with increasing temperature, the advantage that at higher temperatures we will find more reactive species can be cancelled by the fact that the available adsorbed CO will be decreased. In fact different strategies for increasing the sensitivity to CO are based on approaches that will deliver more reactive oxygen species at lower temperatures either by surface doping – that will decrease the activation energy for oxygen dissociation – or by operating the sensors in a pulsed temperature mode – at high temperatures the surface is loaded with reactive oxygen species that, by quenching, are available for the reaction with CO at low temperatures – where the CO adsorption is strong [44].

5. Reaction modelling

Additionally to the facts discussed above, one should consider the following:

- The increase of the annealing temperature of tin dioxide based sensors increases the concentration of the oxygen vacancies at the surface [23,45].
- Although, there is no full agreement between the experimental and the theoretical studies we can assume that an increase of the oxygen vacancies concentration at the surface of tin dioxide determines an increase of the concentration of the ionosorbed oxygen species (O_2^-, as well as of the O^-); oxygen vacancies are considered to be surface sites for oxygen ionosorption [46–48].
- The temperature determines the nature of the oxygen surface species. At a certain operating temperature and oxygen partial pressure, the ratio $[O_2^-]/[O^-]$ is constant for a given surface [49].
- The system is in a steady state condition, so the oxygen adsorption route is unimportant and does not have any influence on the equilibrium concentration of the different forms of oxygen [50].
- The total amount of ionsorbed species cannot exceed the Weisz limitation.
- O^- is a more reactive species than O_2^- [48,51].

All these aspects need to be taken into consideration in any attempt towards the explanation of the effects of the pretreatment temperature on the state of the surface of tin dioxide based sensors. On their basis one can try to assign an electrical effect (Section 4.2) to the spectroscopic findings (Section 4.1).

The higher sensitivity of the sensor T500 can be explained by a more important role of O_2^- in CO sensing; the sensing is mainly due to the processes described by Eqs. (1) and (4). This is demonstrated by the dominance of monodentate carbonates as intermediate species at the surface. We think that this is due to the lower concentration of oxygen vacancies/adsorption sites corresponding to the lower annealing temperature that result in a lower concentration of O^-.

The general decrease of the sensitivity and sensor signal for both types of sensors at 400 °C can be explained, on the one hand, by the dominance of O^{2-} (the sensing is mainly due to the process described by Eq. (6)) for the sensitivity and, on the other hand, by the decrease of the available CO surface concentration.

The highest sensor signal for the sensor T700 is obtained at a lower temperature than the one for the sensor T500 (the sensing is mainly due to the process described by Eq. (2)); this is due to the presence of highly reactive oxygen species (O^-) at lower temperatures for the sensor T700 and demonstrated by the increase of the carboxylates as intermediate species.

On the basis of the actual knowledge we cannot explain the presence of a sensitivity maximum at 300 °C for both types of sensors.

To sum up, we have shown that behind the changes of the sensitivity and sensor signal induced by the change of the sensors' annealing temperature are hidden complex reactions that involve different surface species. Although it is difficult to unambiguously discriminate the particular role of specific surface species in the complex process of CO sensing, one can conclude that most of the experimental data we have, suggest in the case of sensors T500 a dominant CO interaction with O_2^-, while in the case of sensor T700 the reaction with O^- has the major significance for the electrical effects.

6. Summary and outlook

In this work we made an attempt to understand the origin for different CO reaction route at the surface of tin dioxide based sensors determined by the final sensors' thermal treatment. For the first time we managed to identify the underlying reasons of the importance of the annealing process in the sensing performance. We were able to relate the known changes of the concentration of oxygen vacancies, determined by thermal treatment (in our case the final annealing process), to the different reaction paths identified to take place at the surface to the sensors annealed at 500 and 700 °C. We concluded that in fact the final annealing temperature influences the concentration of the reactive site for oxygen ionosorption, which determines the temperature dependence of the distribution of the different oxygen surface species with the final result of changing the main CO reaction route and thus the sensor signal and sensitivity.

The presented model does not take into account surface defects others than oxygen vacancies and the different geometric configurations of the oxygen vacancies, mostly because there are no available studies on heterogeneity of the sites on the surface of thick film tin dioxide sensors and up to date there are only few papers pointing out the role of atomic scale surface defects [52,53].

Acknowledgements

We are indebted to Prof. K. Shimanoe (Faculty of Engineering Sciences, Kyushu University, Fukuoka, Japan) for providing the SnO_2 powder used in this study. The financial support from GOSPEL NoE IST507610 is acknowledged.

References

[1] P.G. Harrison, A. Guest, J. Chem. Soc., Faraday Trans. 83 (1987) 3383–3397.
[2] M.I. Baraton, L. Merhari, Mater. Trans. 42 (2001) 1616–1622.
[3] A. Chiorino, G. Ghiotti, F. Prinetto, M.C. Carotta, G. Martinelli, M. Merli, Sens. Actuators B Chem. 44 (1997) 474–482.
[4] D. Amalric-Popescu, F. Bozon-Verduraz, Catal. Today 70 (2001) 139–154.
[5] T. Armaroli, T. Becue, S. Gautier, Oil Gas Sci. Technol.-Rev. IFP 59 (2004) 215–237.
[6] S. Emiroglu, N. Barsan, U. Weimar, V. Hoffmann, Thin Solid Films 391 (2001) 176–185.
[7] M. Wallin, H. Gronbeck, A.L. Spetz, M. Skoglundh, Appl. Surf. Sci. 235 (2004) 487–500.
[8] J. Trimboli, M. Mottern, H. Verweij, P.K. Dutta, J. Phys. Chem. B 110 (2006) 5647–5654.
[9] J.J. Benitez, M.A. Centeno, C. Louis Dit Picard, O. Merdrignac, Y. Laurent, J.A. Odriozola, Sens. Actuators B Chem. 31 (1996) 197–202.
[10] S. Harbeck, A. Szatvanyi, N. Barsan, U. Weimar, V. Hoffmann, Thin Solid Films 436 (2003) 76–83.
[11] D. Koziej, N. Barsan, V. Hoffmann, J. Szuber, U. Weimar, Sens. Actuators B Chem. 108 (2005) 75–83.
[12] D. Koziej, N. Barsan, K. Shimanoe, N. Yamazoe, J. Szuber, U. Weimar, Sens. Actuators B Chem. 118 (2006) 98–104.
[13] T. Sahm, A. Gurlo, N. Barsan, U. Weimar, L. Madler, Thin Solid Films 490 (2005) 43–47.
[14] J.C. Lavalley, Catal. Today 27 (1996) 377–401.
[15] N. Barsan, U. Weimar, J. Phys.-Condens. Matter 15 (2003) R813–R839.
[16] M. Bauer, N. Barsan, K. Ingrisch, A. Zeppenfeld, I. Denk, B. Schuman, U. Weimar, W. Göpel, in: Proceedings of the 11th European Microelectronic Conference, Venice, Italy, (1997), pp. 37–44.
[17] A. Chiorino, G. Ghiotti, M.C. Carotta, G. Martinelli, Sens. Actuators B Chem. 47 (1998) 205–212.
[18] S. Saukko, U. Lassi, V. Lantto, M. Kroneld, S. Novikov, P. Kuivalainen, T.T. Rantala, J. Mizsei, Thin Solid Films 490 (2005) 48–53.
[19] M.I. Baraton, L. Merhari, H. Ferkel, J.F. Castagnet, Mater. Sci. Eng. C-Biomimetic Supramol. Syst. 19 (2002) 315–321.
[20] S. Lenaerts, J. Roggen, G. Maes, Spectrochim. Acta 51A (1995) 883–894.
[21] M.I. Baraton, L. Merhari, Rev. Adv. Mater. Sci. 4 (2003) 15–24.
[22] N.S. Baik, G. Sakai, N. Miura, N. Yamazoe, Sens. Actuators B Chem. 63 (2000) 74–79.
[23] C. Kittel, Introduction to Solid State Physics, John Wiley & Sons, Inc., 1986, pp. 515–618.
[24] F. Gaillard, M. Abdat, J.P. Joly, A. Perrard, Appl. Surf. Sci. 238 (2004) 91–96.
[25] J. Kappler, N. Barsan, U. Weimar, A. Dieguez, J.L. Alay, A. Romano-Rodriguez, J.R. Morante, W. Gopel, Fresenius J. Anal. Chem. 361 (1998) 110–114.
[26] A. Dieguez, A. Romano-Rodriguez, J.L. Alay, J.R. Morante, N. Barsan, J. Kappler, U. Weimar, W. Gopel, in: Proceedings of the Seventh IMCS, Bejing, 1998.
[27] S. Samson, C.G. Fonstand, J. Appl. Phys. 44 (1973) 4618–4621.
[28] N. Yamazoe, J. Fuchigami, M. Kishikawa, T. Seiyama, Surf. Sci. 86 (1979) 335–344.
[29] J. Maier, W. Goepel, J. Solid State Chem. 72 (1988) 293–302.
[30] N. Sergent, P. Gelin, L. Perier-Camby, H. Praliaud, G. Thomas, Sens. Actuators B Chem. 84 (2002) 176–188.
[31] D.A. Popescu, J.M. Herrmann, A. Ensuque, F. Bozon-Verduraz, Phys. Chem. Chem. Phys. 3 (2001) 2522–2530.
[32] J. Zhang, L. Gao, J. Solid State Chem. 177 (2004) 1425–1430.
[33] S. Bratos, H. Ratajczak, J. Chem. Phys. 76 (1982) 77–85.
[34] A. Zecchina, S. Bordiga, G. Spoto, D. Scarano, G. Spano, F. Geobaldo, Chem. Soc., Faraday Trans. 92 (1996) 4863–4875.
[35] Ü. Kersen, L. Holappa, Anal. Chim. Acta 562 (2006) 110–114.
[36] M. Che, A.J. Tench, Adv. Catal. 31 (1982) 40–42.
[37] N. Barsan, U. Weimar, J. Electroceram. 7 (2001) 143–167.
[38] V.F. Kiselev, O.V. Krylov, Adsorption and Catalysis on Transition Metals and Their Oxides, Springer, 1989, pp. 240–242.
[39] A.A. Davydov (Ed.), Molecular Spectroscopy of Oxide Catalyst Surfaces, John Wiley & Sons Ltd., 2003, pp. 134–139 (and references therein).
[40] D. Koziej, N. Barsan, V. Hoffmann, J. Szuber, U. Weimar, in: Proceedings of the IV Semiconductor Gas Sensors Conference, Ustron, Poland, 2004.
[41] W. Schmid, Consumption measurements on SnO_2 sensors in low and normal oxygen concentration, Ph.D., Eberhard-Karls University, Tübingen, 2004.
[42] D. Koziej, N. Barsan, U. Weimar, J. Szuber, K. Shimanoe, N. Yamazoe, Chem. Phys. Lett. 410 (2005) 321–323.
[43] K.W. Van Every, P.R. Griffiths, Appl. Spectrosc. 45 (1991) 347–359.
[44] N. Bârsan, U. Weimar, in: S. Nakata (Ed.), Chemical Analysis Based on Nonlinearity, Nova Science Publishers, Inc., New York, 2003, pp. 68–77.
[45] A. Vancu, R.B.N. Ionescu, P.C.A.S. Middelhoek (Eds.), Thin Film Resistive Sensors, IOP Publishing Ltd., 1992, pp. 437–491.
[46] M. Menetrey, A. Markovits, C. Minot, G. Pacchioni, J. Phys. Chem. B 108 (2004) 12858–12864.
[47] J.W. Erickson, S. Semancik, Surf. Sci. 187 (1987) L658–L668.
[48] J.H. Lunsford, Catal. Rev. 8 (1973) 135–157.
[49] M.J. Madou, S.R. Morrison, Chemical Sensing with Solid State Devices, Academic Press, Inc., 1988.
[50] F.F. Wolkenstein, Electronic Processes On The Surface Of Semiconductors During Chemisorption, Consultants Bureau, New York, 1991.
[51] S.R. Morrison, The Chemical Physics of Surfaces, Plenum Press, New York, 1990.
[52] M. Batzill, U. Diebold, Prog. Surf. Sci. 79 (2005) 47–154.
[53] K.N. Yu, Y.H. Xiong, Y.L. Liu, C.S. Xiong, Phys. Rev. B 55 (1997) 2666–2671.